JOURNAL OF MATERIALS SCIENCE 27 (1992) 1391–1396

Influence of microstructure on the hydrogen embrittlement of Al–Li–Cu–Mg–Zr alloys

E. QUADRINI, P. MENGUCCI*
*Department of Mechanics, and *Department of Materials Science, University of Ancona, Via Brecce Bianche, I-60131, Ancona, Italy*

The effects of microstructure and hydrogen charge time on the delayed fracture of the AA 8090 Al–Li alloy have been studied using fracture tests and TEM techniques. The results obtained from the fracture tests showed that the solubilization heat treatment confers the lowest hydrogen sensitivity on the alloy which increases with the hydrogen discharging time, and the hydrogen embrittlement sensitivity increases with the ageing time and reaches a maximum at 90 h. This behaviour was attributed to the interaction of the mobile dislocations, which are responsible for the hydrogen transportation, with phases precipitated during the ageing treatment.

1. Introduction

The great interest caused by the introduction of the Al–Li alloy, with respect to the traditional high-strength aluminium alloys, is mainly due to the possibility of achieving structures considerably lighter after suitable redesigning. It is known that for each per cent in weight of lithium, the alloy's density is reduced by 3%, whereas the elastic modulus is increased by 6%. However, for successful application of Al–Li alloys, it is also important to understand the effect of aggressive environments, such as salt water and humid air, on the mechanical properties of these alloys. Previous studies indicate that Al–Li alloys are generallly susceptible to stress corrosion cracking [1, 2], and that hydrogen plays an important role in this process in Al–Li alloys as well as in other traditional high-strength aluminium alloys [3–5].

Lithium is a very reactive element and its addition is unfavourable in corrosion resistance. Moreover, the precipitation of the δ-Al–Li phase on grain boundaries decreases the stress corrosion cracking resistance [6, 7]. It is also known that lithium increases the sensitivity to localized corrosion and, in particular, pitting corrosion [8]. Furthermore, hydrogen embrittlement tends to be increased by the addition of lithium due to reaction with hydrogen. The object of the present study was to examine the effects of microstructure and hydrogen concentration on the tensile properties of AA 8090 Al–Li alloy. Hydrogen was introduced into the samples by means of a cathodic charge using a 0.04 N HCl solution.

2. Experimental procedure

The material used in the present study was industrial 8090 T8X25 (solution treated, water quenched, stretched 2%, aged 12 h at 135 °C). The nominal composition and mechanical properties of the alloy are shown in Tables I and II, respectively.

The alloy's microstructure is characterized by columnar arrays of small, recrystallized grains and stringer particles lying parallel to the longitudinal axis of the bar (extrusion direction), as shown in Fig. 1.

Plate-type tensile specimens, with 24 mm gauge length and 3 mm thick, were machined from the mid-section of the plate in order to obtain a tensile orientation parallel to the rolling direction.

The samples were treated in an anhydrous argon atmosphere at a temperature of 520 °C for 8 h and then quenched in a brine bath at 0 °C. This procedure not only dissolved existing precipitates in the samples, but also annealed any mechanically deformed surface layer resulting from the machining and polishing operations.

In order to obtain a different microstructure after solution treatment, some specimens were aged in a thermostatically controlled silicone-based bath at 160 ± 1 °C for times ranging from 10 min–90 h.

Fig. 2 shows the values of hardness as a function of ageing time. This operation was carried out in a double-walled glass cylinder in whose cavity the thermostatic liquid circulated. All the specimens were mechanically and chemically polished to remove any surface damage. Hydrogen was introduced into the material using the cathodic loading procedure, with a dilute 0.04 N HCl solution in contact with the atmosphere. The sample which made up the cathode was assembled inside the cylinder, while a platinum coil wrapped round it at a distance of 20 mm acted as a counter-electrode. The effects of hydrogen concentration were studied on heated and water-quenched samples [9, 10]. In these tests the hydrogen charging time was varied from 5 min–16 h.

0022–2461

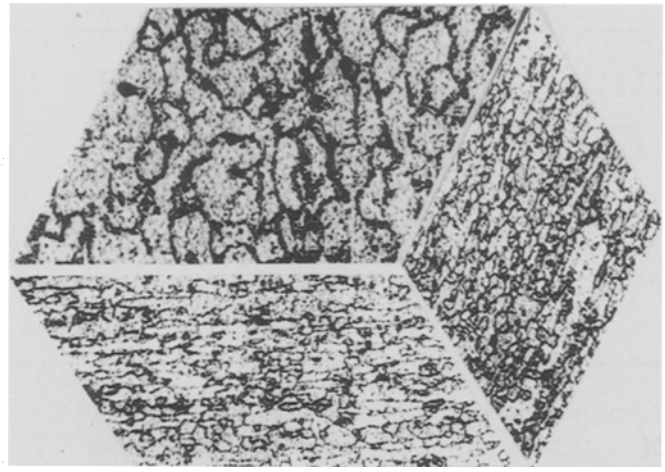

Figure 1 Tri-planar optical micrographs of the alloy's microstructure. Etched with Barker reagent and illuminated by polarized incident light.

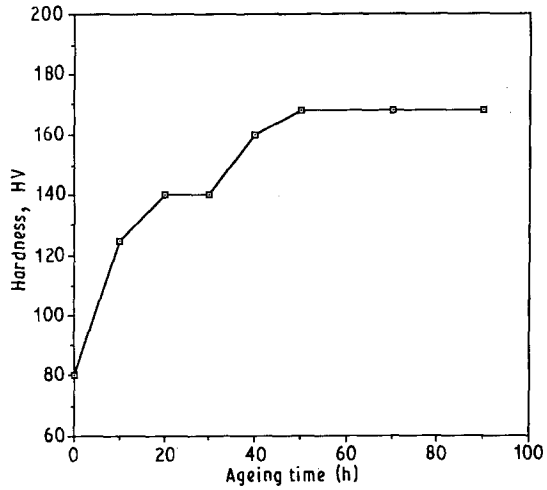

Figure 2 Summary of the hardness–time curves for samples aged at different times.

TABLE I Chemical composition (wt %) of the alloy used

Li	Cu	Mg	Zr	Ti	Fe	Si
2.0	1.9	1.5	0.09	0.03	0.05	0.03

TABLE II Mechanical properties of the alloy used

Rolling direction	RO2 (MPa)	RM (MPa)	A (%)
Longitudinal	425	497	11
Transverse	379	507	19

Tensile specimens were cathodically charged with hydrogen and tested under different load rates. The charging current density employed was 50 mA cm^{-2}. After hydrogen charging, the specimens were tested immediately, in order to minimize the loss of hydrogen. Tensile tests were carried out on an Instron servo-hydraulic testing machine at 20 °C and at a travel speed of 0.042 mm s^{-1}.

The hydrogen embrittlement sensitivity was evaluated from ductility loss measured as follows:

$$ef_{loss} = \frac{ef - ef_H}{ef} \quad (1)$$

where ef and ef_H are the elongations of uncharged and charged specimens, respectively. The microstructure was examined by optical and TEM microscopy.

3. Results and discussion

3.1. TEM observation

TEM analyses were carried out on 3 mm diameter discs mechanically thinned with grinding papers. Final thinning was performed in a double-jet unit using a 30% HNO_3–methanol solution at −40 °C and 12 V. A TEM Philips CM 12 equipped with a LaB_6 cathode at 120 kV was used.

Observations on samples aged at 160 °C from 10 min–90 h showed the presence of the δ′-Al_3Li metastable coherent phase and of the Al_3Zr dispersoids in all the specimens investigated. Dispersoids precipitate during the homogenization process of the alloy and act as an anti-recrystallizing phase. Under appropriate diffraction conditions it is possible to show evidence of the δ′ ring surrounding the Al_3Zr phase.

In the solution-treated specimen, the spherical coherent δ′ phase precipitates as a consequence of the oversaturation of vacancies during quenching. Fig. 3a shows the fine dispersion of this phase in the as-quenched sample. Dispersoids surrounded by an Al_3Li ring are also evident. Heat-treated samples exhibit a coarsening with time of the δ′ phase which contributes, in this way, to the hardening of the alloy. The coarsening sequence is shown in Fig. 3 for three different tempers. The micrographs are dark-field images taken with a δ′ superlattice spot. Matrix orientation is ⟨0 0 1⟩, as shown from the diffraction pattern. Specimens aged for 90 h exhibit, in addition to the dispersoids and δ′ phase, the metastable S′-Al_2CuMg needle-like phase which nucleates both homogeneously inside grains and heterogeneously on dislocations and grain boundaries. In Fig. 4, S′ precipitates homogeneously nucleated inside a grain are shown. The dark-field image evinces the tendency of the precipitate to nucleate on the coarsened δ′ particles.

Heterogeneous nucleation on a grain boundary and on dislocations of the S′ phase is shown in Fig. 5. Coarse precipitates of T2-$Al_6Cu(Li, Mg)_3$ phase were observed in all tempers. They exhibit five-fold diffraction symmetry and are always segregated at grain

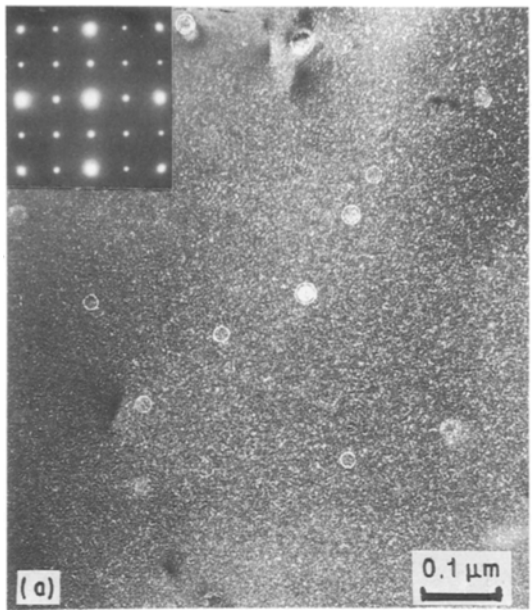

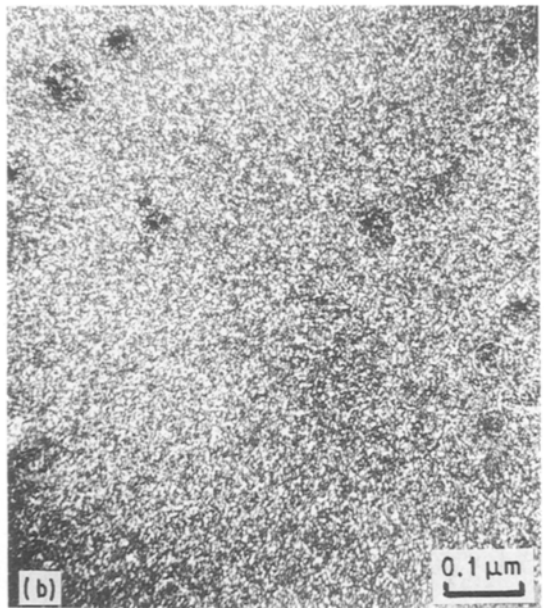

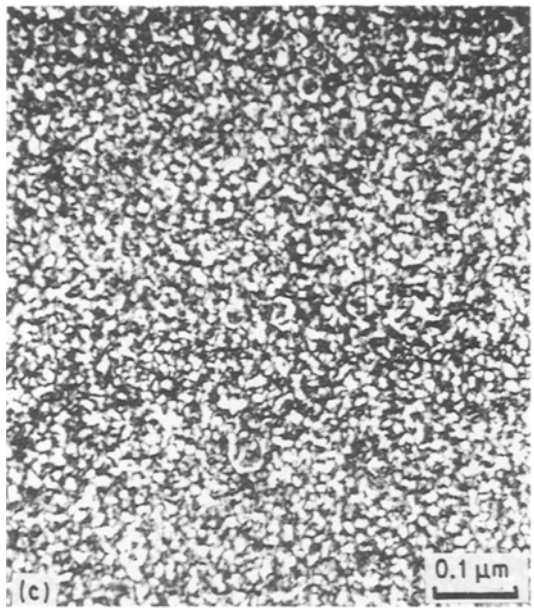

Figure 3 TEM dark-field images showing the distribution and coarsening of δ′ phase after quenching and heating at 160 °C: (a) as-quenched, (b) 10 min and (c) 90 h aged samples.

boundaries. They probably form during the production of the alloy, as can be inferred from their non-uniform distribution.

3.2. Effect of hydrogen concentration

Fig. 6 shows the evolution of ductility loss in relation to the hydrogen charging time. Each data point indicates the average of the results obtained from at least four different specimens tested under identical testing conditions. The curve's trend shows a considerable variation of the tensile properties under the charging conditions employed in the present study. In particular, a maximum in the proximity of 20 min is shown.

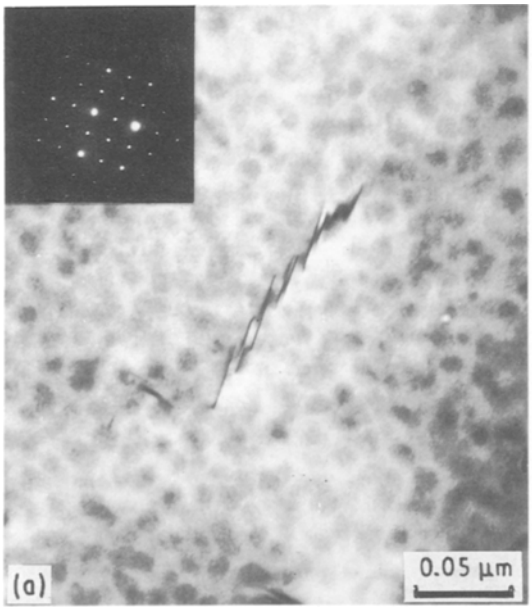

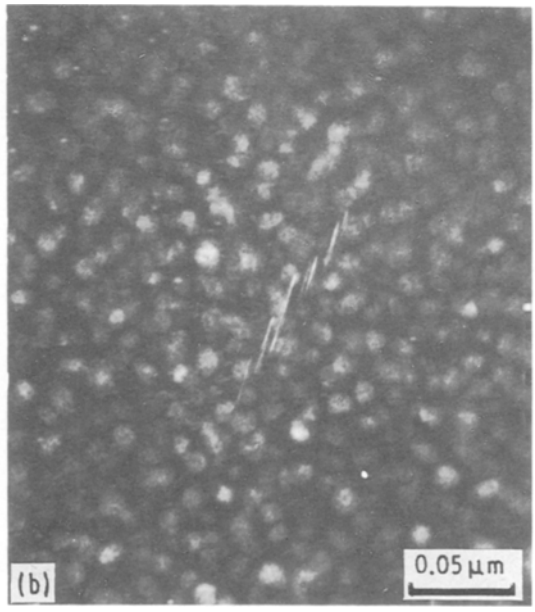

Figure 4 S′ precipitates homogeneously nucleated inside a grain after 90 h at 160 °C: (a) bright-field and (b) dark-field images of the same zone.

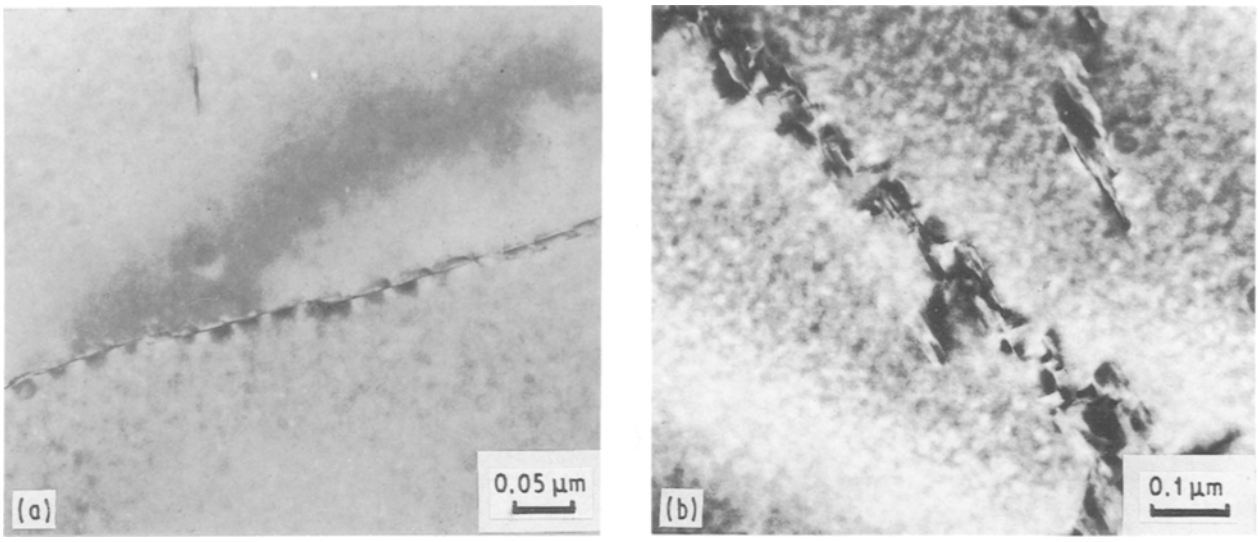

Figure 5 S′ heterogeneously nucleated (a) on a grain boundary and (b) on dislocations. Specimen aged at 160 °C for 90 h.

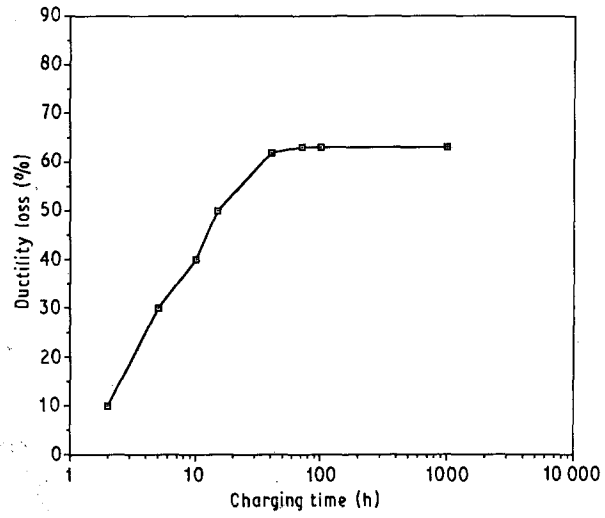

Figure 6 Effect of charging time on the ductility loss.

This time can be considered, with good approximation, as the time necessary for our samples to reach maximum hydrogen concentration.

In order to explain this behaviour, we must consider the phenomena which occur in the material during plastic deformation. As a consequence of the deformation, stress relaxation phenomena are induced in the crack tip. During these deformations, cavitation phenomena occur in the sites in which local stress reaches the critical value and, consequently, there is a release of tension at the crack tip. In this way, during load application there is an increase both in the microvoid population and in sites with subcritical stress values. Some of these sites have a value very close to the stress necessary to cause cavitation.

Some authors suppose [9, 10] that during the initial relaxation phenomenon the number of subcritically stressed sites decreases with time. If the material is already saturated with hydrogen when these relaxation phenomena occur, the sites which in the absence of hydrogen were under subcritical stress, in the presence of hydrogen reach critical stress with subsequent nucleation of microvoids, because of the decrease in local cohesive strength. The presence of these microvoids, facilitates hydrogen diffusion in front of the crack tip, thus decreasing in these sites the mechanical resistance of the material facilitating the fracture. Therefore it is evident that with a higher hydrogen concentration during load application, there is a corresponding higher number of microvoids, which from being subcritically stressed, then become critically stressed, making the material much more sensitive to hydrogen-induced fracture.

3.3. Effect of microstructure

The results of the effect of hydrogen on yield strength, ultimate tensile strength and elongation after fracture are reported in Table III.

Fig. 7 shows the evolution of ductility loss in relation to the ageing time. The values reported show a sensitive increase in hydrogen embrittlement susceptibility with ageing time. This susceptibility reaches a maximum at 90 h. This behaviour can be attributed to the interactions between different phases precipitated during the ageing treatment and the hydrogen transported by dislocations. The hydrogen can be trapped not only by mobile defects such as dislocations, but

TABLE III Effect of hydrogen on yield strength (YS), ultimate tensile strength (UTS) and elongation to fracture (El)

Ageing time (h)	Conditions	YS (MPa)	UTS (MPa)	El (%)
2	Charged	411	479	8.2
	Uncharged	390	450	6.4
10	Charged	471	507	6.0
	Uncharged	444	480	4.8
30	Charged	481	518	3.1
	Uncharged	448	470	2.1
50	Charged	492	526	4.1
	Uncharged	450	475	2.5
70	Charged	510	556	4.0
	Uncharged	472	490	1.3
90	Charged	530	560	4.0
	Uncharged	475	503	1.2

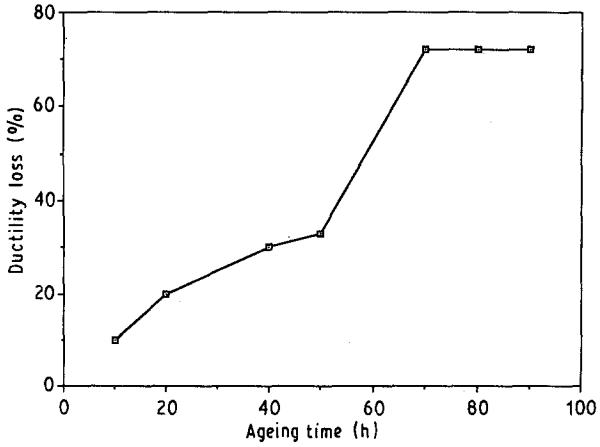

Figure 7 Effect of ageing time on the ductility loss.

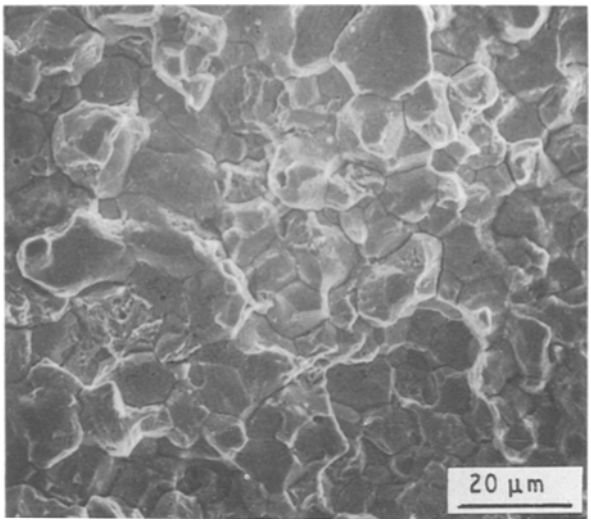

Figure 8 SEM fractograph showing predominantly ductile fracture.

also by vacancies, voids and interstitial atoms which are static traps. In contrast with the delaying effect induced by such traps when they are static, an opposing "accelerating" effect may occur whenever such traps are put into motion. Several models in the literature have examined such situations [11–13] for the case of hydrogen transported by dislocations, which is expected to differ from interstitial diffusion in the following ways. Dislocations will transport more hydrogen with respect to the same length of a normal diffusion front. Estimates [14, 15] give 10^4 times more hydrogen transported by dislocations than by the lattice (up to 10^7 H atoms/cm). However, such values are sensibly modified by phases precipitated during heat treatments. In particular, the S′-Al_2CuMg phase which appears at 90 h ageing time, nucleates heterogeneously close to dislocations, becoming an efficient trap for the hydrogen transported by dislocations. Therefore, the zones where the S′ phase nucleates, will reach the hydrogen critical concentration in a shorter time rendering a material much more sensitive to hydrogen-induced fracture.

The fracture surfaces of most specimens, both hydrogenated and unhydrogenated, were examined by SEM and the fracture surfaces are shown in Figs 8 and 9. On the uncharged specimens, the resulting fracture

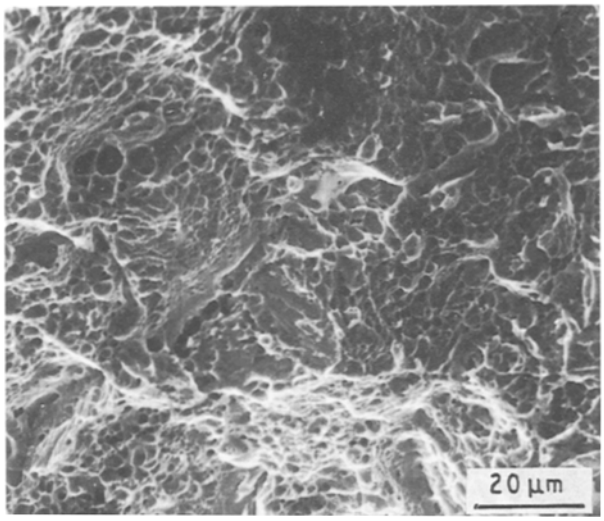

Figure 9 SEM fractograph showing intergranular fracture.

morphology is prevalently ductile (Fig. 8), while on the specimens aged for 90 h the resulting morphology is mainly intergranular (Fig. 9). This morphology is typical of brittle hydrogen-induced fracture.

4. Conclusions

Hydrogen embrittlement of the AA 8090 Aluminum alloy was studied at different hydrogen charging times and ageing treatments.

With increasing hydrogen charging time the alloy shows a greater susceptibility to hydrogen-induced fracture. This behaviour was attributed to the interaction between the hydrogen atoms and the microvoids nucleated during deformation.

A greater susceptibility of the alloy to the hydrogen-induced fracture was also observed on increasing the ageing time.

The maximum sensitivity is exhibited by 90 h aged specimens. This behaviour was attributed to the S′ phase which slows down the mobility of dislocations and constitutes an efficient trap for the hydrogen atoms. These specimens show a brittle surface fracture.

References

1. R. C. DORWARD, *Mater. Sci. Engng* **84** (1986) 89.
2. R. J. GESZT and A. R. TROIANO, *Corrosion* **30** (1974) 274.
3. J. ALBRECHT, B. J. McTIERNAM, I. M. BERNSTEIN and A. W. THOMPSON, *Scripta Metall.* **11** (1977) 893.
4. P. NISKANEN, T. H. SANDERS Jr, J. G. RINKER and H. MAREK, *Corrosion* **22** (1982) 283.
5. R. E. RICKER and D. J. DUQUETTE, in "Proceedings of the 2nd Al–Li Conference", edited by T. H. Sanders Jr and E. A. Starke Jr (The Metallurgical Society of AIME, Warrendale, PA, 1983) p. 581.
6. M. AHAMAD, *J. de Phys.* **9** (1987) 871.
7. E. I. MELETIS, *Mater. Sci. Engng* **93** (1987) 235.
8. S. SCHNURIGER, G. MANKOWSKI, Y. ROQUE, G. CHATAINIER and F. DABOSI, in "4th International Aluminum–Lithium Conference", Vol. 9, edited by G. Champier, B. Dubost, D. Miannay and L. Sabetay (Les Editions de Physique, Les Ulis Cedex, France, 1987) p. 853.

9. J. ALBRECHT, A. W. THOMPSON and I. M. BERNESTEIN, *Metall. Trans.* **10** (1979) 1759.
10. D. A. HARDWICK, M. THAERI, A. W. THOMPSON and I. M. BERNSTEIN, *ibid.* **13A** (1982) 235.
11. M. IINO, *Acta Metall.* **30** (1982) 367.
12. G. M. PRESSOUYRE, *ibid.* **28** (1980) 895.
13. J. P. HIRTH, *Metall. Trans.* **11A** (1980) 861.
14. E. QUADRINI, *J. Mater. Sci.* **24** (1989) 915.
15. G. M. PRESSOUYRE, J. DOLLET and V. B. BARON, *Neveu Metall.* **79** (1982) 161.

Received 15 January
and accepted 7 June 1991